The new international reference system for pure alpha- and pure beta-emitting radionuclides and some electron capture decaying radionuclides by liquid scintillation counting

Romain Coulon, Ryszard Broda, Philippe Cassette, Sammy Courte, Aldo Dupire, Vincent Gressier, Simon Jerome, Steven Judge, Karsten Kossert, Haoran Liu, et al.

The new international reference system for pure alpha- and pure beta-emitting radionuclides

Romain Coulon[1], Ryszard Broda[2], Philippe Cassette[3*], Sammy Courte[1], Aldo Dupire[1], Vincent Gressier[1], Simon Jerome[4], Steven Judge[1*], Karsten Kossert[5], Haoran Liu[6], Carine Michotte[1], Manuel Nonis[1]

[1]*Bureau International des Poids et Mesures, Pavillon de Breteuil, F-92312 Sèvres Cedex, France*

2 National Centre for Nuclear Research Radioisotope Centre POLATOM, 05-400 Otwock, Poland

[3] *Université Paris-Saclay, CEA, List, Laboratoire National Henri Becquerel (LNE-LNHB), F-91120 Palaiseau, France*

[4] *Norges miljø- og biovitenskapelige universitet (NMBU), 1433 Ås, Norway*

[5] *Physikalisch-Technische Bundesanstalt (PTB), Bundesallee 100, 38116 Braunschweig, Germany*

[6] *National Institute of Metrology (NIM), 100029 Beijing, China*

* *Now retired.*

E-mail address of the corresponding author: romain.coulon@bipm.org

Abstract

The Bureau International des Poids et Mesures (BIPM) is developing with the support of national metrology institutes an extension to the existing international reference system of radionuclide metrology to address pure alpha-, pure beta-emitting and some electron capture-decaying radionuclides. The new service is based on a liquid scintillation counter

and the triple to double coincidence (TDCR) technique. A dedicated facility to prepare liquid scintillation sources and a TDCR system have been set up at the BIPM. The TDCR system was conceived and commissioned in order to ensure the long-term reproducibility of the reference it produces. The metrology is based on a dedicated approach which uses the TDCR value as a parameter to stabilize the output quantities of the system against changes in detection efficiency or asymmetry that could appear in a long-term period of operation. The quality assurance based on periodic controls of toluene-based liquid scintillation sources of ^{3}H and ^{14}C has permitted to demonstrate the reproducibility of the system for a 20-month period.

Keywords

Radionuclide Metrology, Key comparisons, Liquid scintillation, TDCR, ESIR

1. Introduction

The Bureau International des Poids et des Mesures (BIPM) operates an international reference system (the SIR) to compare standards of radioactivity realized by National Metrology Institutes / Designated Institutes (NMI/DIs), to enable NMI/DIs to demonstrate the equivalence of standards leading to a harmonized international measurement system. The operation of the international measurement system is described in more detail in a Mutual Recognition Arrangement, the CIPM MRA [1,2].

The SIR is a re-entrant ionization chamber; the output value is the ratio of the ionization current measured with the source to be analyzed to the current produced by long-lived sealed sources of ^{226}Ra [3–5]. In practice, the long-term reproducibility and the precision achieved by this relative measurement allow to assess equivalences for most of the gamma-emitting radionuclides. To cope with the increasing demand in nuclear medicine in short-lived gamma-emitting radionuclides (e.g. ^{99m}Tc, ^{18}F, ^{64}Cu, ^{11}C…), a transportable version called the SIRTI is also available [6]. The well-type NaI(Tl) detector operates using as a reference: a long-lived sealed source of ^{94}Nb. It is linked to

the SIR and can travel to laboratories far from the BIPM to obtain equivalences for these radionuclides. The main asset of the SIR/SIRTI services for NIM/DIs is to avoid organizing large-scale comparison exercises implying send radioactive sources around the world. The SIR is an on-demand service which permits the NIM/DIs to obtain equivalence whenever they desire. Moreover, the efficiency in delivering comparison results has been recently enhanced through a new database and automated reporting [7].

There are still some radionuclides that are not covered by the SIR/SIRTI services of the BIPM: pure (or quasi-pure) alpha-particle emitters, pure (or quasi-pure) beta-particle emitters, and some electron-capture decaying radionuclides (such as ^{55}Fe). The ionizing particles emitted during the decay of these radionuclides cannot pass (or very weakly) through the entry windows of the detectors and produce a sufficient signal. Meantime, there is an increasing demand to evaluate equivalence of radioactive standards containing these types of isotopes. New cancer treatments are emerging using radiopharmaceuticals tagged by radionuclides decaying in a way to depose very locally the dose [8–10]. Hence, Targeted Beta-particle Therapy (TBT) and Targeted Alpha-particle Therapy (TAT) aim to efficiently damage cancerous cells while sparing healthy tissues. Radionuclides that are used (or studied to be used) in TBT are for instance: ^{32}P, ^{89}Sr, ^{90}Y, ^{169}Er, ^{177}Lu and the ^{186}Rh. Radionuclides that are used (or studied to be used) in TAT are for instance: ^{225}Ac, ^{211}At, ^{212}Bi, ^{212}Pb, ^{213}Bi, ^{227}Th and the ^{223}Ra. Some of these isotopes, such as the ^{177}Lu used in the theragnostic perspective [11], emits enough x or gamma radiations to be measured by the SIR/SIRTI [12–14]. However, it is not possible for most of them. In addition to that, the need to assess the international equivalence of standards of pure alpha- or beta-emitting radionuclides arises also for environmental issues where for instance ^{89}Sr, ^{90}Y, ^{160}Tb, ^{161}Tb and ^{210}Po are of critical use for nuclear forensics [15–17].

Liquid scintillation counting appears to be the most suitable measurement techniques to address the measurement issue associated with these radionuclides. This is why, the extension of the SIR (called the Extended SIR (ESIR)) is under development since 2018 and based on a liquid scintillation counter and an approach derived from the primary standardization technique called: Triple to Double Coincidence Ratio counting

(TDCR) [18,19]. On contrary to the SIR and SIRTI which achieve a long-term reproducibility using long-lived radioactive sources and a relative measurement, the ESIR implements another way to ensure reproducibility since the long-term stability of a liquid scintillation source cannot be assumed [20] even for the nonaqueous ones (see section 5). So, it has been decided to take benefit from the *TDCR* parameter which is strongly correlated with the detection efficiency of the system to realize a self-stabilization of the system. The output values delivered by the ESIR are comparison indicators, *I*, stabilized using the *TDCR* value in different ways such as:

- I_0 is the non-stabilized comparison indicator,
- I_1 is the comparison indicator stabilized by a 2^{nd} order polynomial function of the *TDCR* value (built for robustness against efficiency changes),
- I_2 is the comparison indicator stabilized by the calculation of an equivalent efficiency based on the TDCR model parametrized by fixed parameters (built for robustness against both efficiency and asymmetry changes),
- I_3 is the comparison indicator obtain by making a monoenergetic assumption in the TDCR model (it can be used for isotopes emitting close-to-monoenergetic particles such as the ^{55}Fe).

Details on the calculation of these ESIR comparison indicators are given in [21–23].

In addition to this unique approach, it is also critical for this new service:

- to develop and maintain a source preparation facility with an accurate mass measurement of active solutions,
- to develop and maintain a TDCR system suitable for long-term operations,

- to develop and maintain a proper associated quality assurance to monitor the long-term reproducibility of the measurement system.

2. The liquid scintillation source preparation facility

To prepare liquid scintillation (LS) sources at the BIPM, aliquotes of an active solution standardized by a laboratory are injected into LS vials containing LS cocktail.

a. The liquid scintillation cocktail

It was decided to use the Ultima-Gold (UG) cocktail from Perkin Elmer – (or equivalent). It pemits to properly disolve the acqueous active solution while providing a good scintillation yield. Ionisation quenching depends strongly on the properties of the LS cocktail and it canot be assumed a perpect reproducibility from batch to batch of UG cocktails. However, as ionisation quenching effects are of relative minor importance for medium and high energy depositions into the LS liquid, it can be assumed that UG (or similar type of cocktails) will fit the purpose for the majority of radionuclides to address.

Nevetheless, the reproducibility of the ESIR when using UG cocktail could remains an issue for low energy-deposited particles encountered for instance during decays of ^{3}H, ^{63}Ni, ^{55}Fe or ^{241}Pu. For these latter ones, the duration of key comparison exercices will be limited to the validity period of a given batch of UG. This option imposes constains on laboratories as they cannot send their solutions when appropriate for them but only when a comparison is planned and during a limited period. The second option to ensure on-going comparisons as it is for the SIR, is to produce a specific LS cocktail at the BIPM under reproducible and sustainable conditions. A prelimary study has permitted, through a factorial design approach, to establish the preliminary composition of an LS cocktail that can be reproducibly realised at the BIPM. The components are notably chosen for not being impacted by the European REACH regulation. Thus, the diisopropylnaphtanlen

entering as a solvent in UG composition is replaced by speudocumen (1,2,4-trimethylbenzene) and the anionic surfactant 4-NPE is replaced by bis(2-ethylhexyl)hydrogene-phosphate. Also, to enhance the stability of the LS source in regards with the variation of PH of active solutions, the primary fluorophore 2,5-diphenyl oxazole (PPO) will be replaced by the more robust $1^{1},2^{1}:2^{4}:3^{1}$-terphenyle (p-terphenyle). Further studies will be realized to continue investigations on this option.

b. The vials

Glass vials will be the default type of vials used in the ESIR. However, as emphasis by the rencent CCRI(II).Fe-55 comparison [24], polythylene or frosted glass vials are better options to adress ^{55}Fe and probably other radionuclides emitting low energy particles. Offering a better diffusion of photons in conformance with the TDCR model, polyehylene vials will be used for ^{55}Fe, ^{63}Ni, ^{3}H and ^{241}Pu.

c. The balance

The balance is a Mettler Toledo XPE26C set on a marble table (see Fig. 1). It is recalibrated each year by Mettler Toledo in compliance with the EURAMET calibration guide N°18 [25]. The standard uncertainty for metalic mass in the range from 1 mg to 100 mg is equal or better than 5 µg.

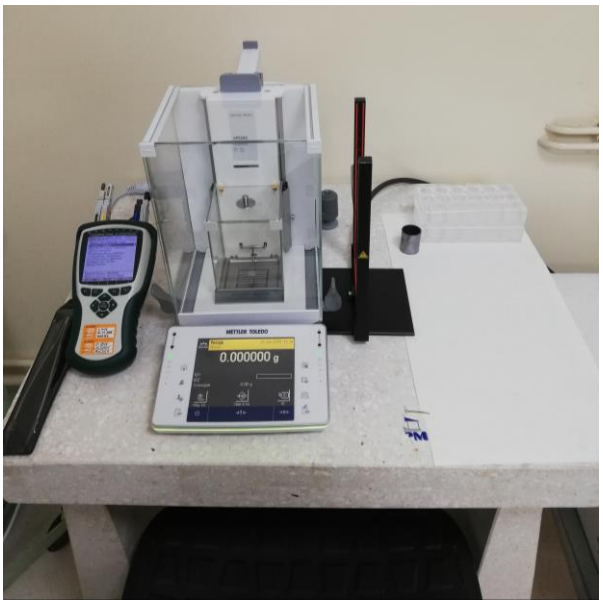

Fig. 1 Photography of the BIPM balance

The differential weighing technique [26] is used to measure the mass of solution put in the vials. The active solution is transfered to a pycnometer which is measured before and after having released some droplets into the vials. One difficulty observed when weighing pycnometers is the electrostatic perturbance from the dielectric material. To cope this issue, a electrostic dicharger is set at the entrance of the balance to remove chages from the pycnomter. Also, prior to each source preparation, blank weighings (without droplet release) of the pycometer is realized to control that the reproducibity is contaitned within +/- 10 µg.

The facility operates for producing LS sources of beta-emitting radionuclides but canot adress alpha-emitting radionuclides. Indeed, the handling of the latter is only allowed within a fume hood whatever the source activity is. The setup of a new balance in a fume hood is in project to enable alpha-emitting radionuclides to be adressed by the ESIR.

d. The sources

10 LS sources are realized for each ESIR submission. The amount of standard solution injected into each vials is calculated so that the double coincidence count rate r_D is

between 5 x 10^3 s^{-1} and 10^4 s^{-1}. This constrain will guaranty to achieve a good counting statistic and to operate the system always in the same range of counting dead time.

It is important to note that it is asumed that the LS sources are not stable. So, it is stated in the procedure that the TDCR measurements must be done within the week just after the source preparation.

3. The TDCR system

The TDCR system of the ESIR is presented in Fig. 2.

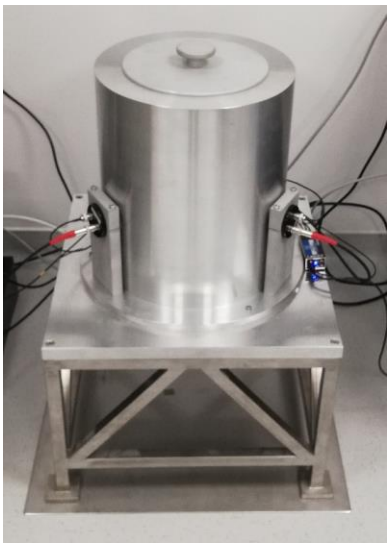

Fig. 2 Photography of the ESIR TDCR system

As any TDCR system, it is composed of:

- a mechanical structure,
- an optical cell,
- a photo-conversion device using 3 photomultiplier tubes (PMTs),
- a specify signal processing electronics.

Technological options for these elements must be specified to address long-term reproducibility and maintainability. To this end, an effort is made to maximize the detection efficiency (close to 1) to minimize the part of the method in the long-term reproducibility strategy. This property is particularly of importance for isotopes emitting low energy particles such as ^{3}H, ^{63}Ni, ^{55}Fe, ^{241}Pu because the model from which I_1, I_2 and I_3 were conceived comes close to its limits to describe the underlying physics due notably to low photoconversion statistics, significance of the ionization quenching, delayed fluorescence, etc. Also, materials and electronics must be chosen in a way to guaranty the sustainability of the reference produced by the system even when parts of the equipment are damaged or come to obsolescence.

a. The mechanical structure

Unlike many TDCR systems, it was chosen not to implement a fourth gamma-rays channel or an embedded source of ^{241}Am for Compton coincidence feature. These options gives the possibility of performing $4\pi(LS)\beta$–γ counting [27] or Compton source efficiency tracing [28]. Another TDCR system will be dedicated for these options because it is preferable for the ESIR to simplify the design as much as possible to meet our specific need exclusively. Thus, the absence of a fourth gamma-rays channel permit to setup a 10 cm-thick gamma-rays shielding with a greater spherical coverage and therefore a lower background noise. Also, the implementation of an ^{241}Am sealed source for Compton coincidence requires coring a collimator hole through the optical cell. The absence of this feature optimizes the symmetry (120° angular spacing between PMTs) of the system. This optimizes the relevance of the I_1 indicator (not implementing asymmetry correction) and minimizes the stabilization effort carried out by the I_2 comparison indicator to maintain reproducible output values under possible asymmetry.

The assembly is placed on a reinforced support and incorporated into a cylindrical steel cover ensuring light tightness. All this mechanical structure was designed and machined at the BIPM workshop. Fig. 3 shows the exploded view of the BIPM TDCR system.

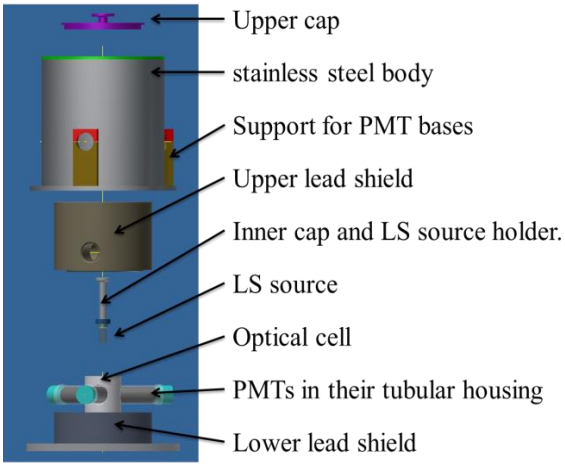

Fig. 3 Exploded view of the BIPM TDCR system

b. The optical cell

It was decided to machine the optical cell in low density PTFE (Gigahertz-Optik ODM98-B [29]). This material, used by the PTB in one of their TDCR systems, has a very good reflectivity (98%) for visible photons. Moreover, this material is also known for its great immunity to chemical attacks and to radiation damages [30]. Therefore, it gives the TDCR system a greater long-term stability of the optical properties than traditional painting of titanium oxide, which requires to be periodically renewed. The optical cell (presented in Fig. 4) has been machined at the BIPM workshop. Like the photocathodes, the internal surfaces of the optical cell are frosted to maximize the stochastic scattering of photons in accordance with the TDCR model.

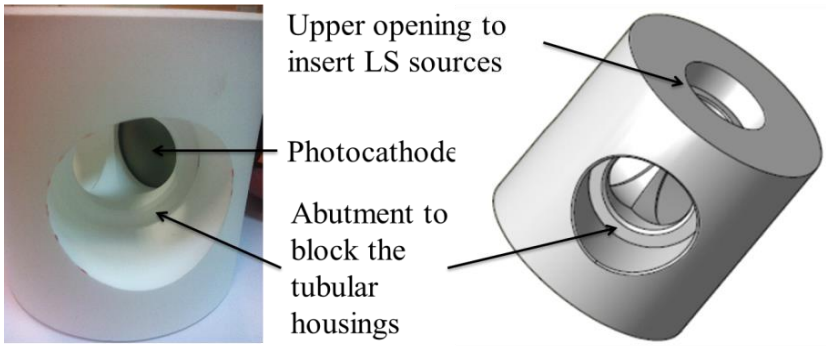

Fig. 4 Photography and 3-D drawing of the optical cell

c. The photoconversion device

The insertion of PMTs through the shield to reach the optical cell is a delicate point where light leaks can occur. To cope with this problem, a tube adjusted to the diameter of the tubular housings of the PMTs has been conceived (see Fig. 5a). This tube comes to lock in abutment of the optical cell so that the photocathode penetrates therein. The PMT is fixed in the tubular housing thanks to an O-ring (see Fig. 5b).

(a) (b)

Fig. 5 Tubular housing of PMT tubes. (a) with a PMT inserted; (b) empty housing showing the O-ring

The PMTs are Hamamatsu R331-05 selected to have an identical quantum efficiency of +/- 1 % for an excitation at the wavelength of 420 nm. As can be seen in Fig. 5a, the bialkali photocathodes are curved and frosted in order to respectively maximize the optical efficiency and the stochastic diffusion of fluorescence photons. The curvature allows the photocathode to approach the LS source borders within 2 mm. Furthermore, the window material is low K content to minimize background noise. Before being inserted into its tubular housing, the PMT is covered with a mu-metal foil to limit the impact of possible electromagnetic disturbances on electron multiplication. The cathode is polarized with a positive voltage. And, in accordance with our strategy to avoid

dispensable features which could be sources of disturbance for the reference to be produced, no potentiometric defocusing has been implemented.

d. The LS source positioning system

The previous BIPM TDCR system used an extruded base at the bottom of the cell to position the source. This approach turns out to have the following two disadvantages:

- having a LS source off-center from the axis of the photocathodes that is not optimal to maximize the detection efficiency,
- achieving in practice mediocre reproducibility of the positioning of the LS source.

For the new system, a special plug has been designed to hold the LS source in a reproducible position maximizing the detection efficiency. The source volume is maintained in the axis of the photocathodes using a jaw build in PTFE which grab the caps of the LS vials (see Fig. 6). This approach is implemented within POLATOM's TDCR systems and gives hope for an almost perfect reproducibility of the positioning of the source.

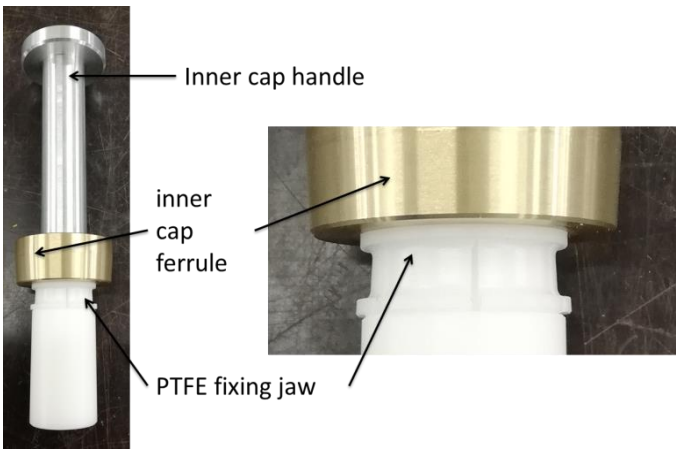

Fig. 6 Photography of the inner cap of the BIPM TDCR system handling a LS source

e. The electronics

The PMTs are polarized at a voltage equal to +2500 V using NHQ103M HV units. This voltage value is ideal to enable the system to detect properly single photoelectron events. The anode signals from the three PMTs are processed by the nanoTDCR module [31,32] (see **Fig.** 5). It embeds in its FPGA the same extended dead time processing as in the reference MAC3 unit [33] which is unfortunately no more maintained. The nanoTDCR provides the following quantities:

- the triple coincidence count rate r_T,
- the logical sum of the double coincidence count rate r_D,
- the double coincidence count rates r_{AB}, r_{BC}, r_{AC} of each pair of the three channels A, B and C.
- the count rates r_A, r_B, r_C from channels A, B and C.

Fig. 7 Photography of the nanoTDCR module

The key comparison indicators of the ESIR are built from these quantities such as:

- I_0 only uses r_D,
- I_1 uses r_D, the *TDCR* value, R_T/R_D, plus two preset parameters α_1 and α_2,

- I_2 uses r_D and the *TDCR* values, R_T/R_{AB}, R_T/R_{BC}, R_T/R_{BC}, plus preset parameters for the TDCR model: the Birks constant *kB*, the stopping power *dE/dx(E)* and the energy spectrum *S(E)*,

- I_3 uses r_T, r_{AB}, r_{BC}, r_{AC}.

The count rates r_A, r_B, r_C are used to correct the measurement from accidental coincidences [34]. Details are available in [35].

To enhance the long-term maintainability of the ESIR, a redundant electronic based on the CEAN digitizer DT5730S is planned to be setup. The list mode data acquisition will permit to have more control on the algorithmic implemented for the TDCR signal processing.

4. Commissioning of the TDCR system

The ESIR aims to produce a fixed reference. So it is of importance that parameters used in the signal processing are defined once and for all. The extended dead time algorithm requires the following parameters:

- The discrimination thresholds on each channel,

- The extended dead time period,

- The coincidence resolving time.

One interesting feature of the nanoTDCR is to process the signal with two different extended dead times and two different resolving times. The setup of these signal processing parameters is described below.

a. Setup of the discrimination thresholds

Fig. 8 presents the pulse high spectra recorded without LS sources in the TDCR system. The left component comes from the thermal electronic noise and the spread peak centred

on about 1 V is induced by the dark noise related to the stochastic thermionic emission from photocathodes. The three spectra as almost superimposed which means that PMTs displayed equivalent thermal noise magnitude and voltage gain. The first set step is to set the discrimination threshold in the valley of the spectra in order to maximize the signal to noise ratio, i.e., minimizing the thermal noise impact while maximizing the detection probability of single electron pulses. According to the shape observed in Fig. 6, thresholds are therefore set at -200 mV for all the 3 channels A, B and C.

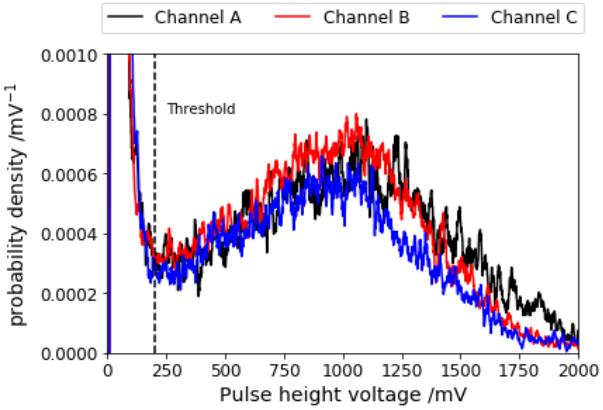

Fig. 8 Pulse high spectra of single photoelectron pulses from the tree channels of the TDCR system

b. Setup of the extended dead time

After-pulses induce a metrological challenge in every measurement systems implementing PMTs [36]. To limit after-pulses impact, the extended dead time method paralyzes the signal processing during an imposed period Δt after each triggering occurring on one of the three channels.

Considering a resolving time set to 50 ns, the TDCR value was estimated as a function of the extended dead time period Δt for 2 toluene-based standard sources of ^{3}H (3.2 kBq) and ^{14}C (2.0 kBq) and presented in Fig. 9. The influence of after-pulses on the measurement seems to be a function of the energy of the beta particles and therefore of the amplitude of the primary pulse. No significant impact is observed in the case of tritium and a Δt of 5 µs seems sufficient for ^{14}C sources to filter this type of disturbance.

To maximize the statistical precision of the counting and the accuracy of the live-time estimation, the dead time of the measurement must be minimized. Thus, by taking a reasonable safety margin, a first Δt equal to 10 µs will ensure after-pulse filtering while minimizing the dead time. The second Δt is set equal to a larger value, 50 µs, and will permit to compare measurement results obtained with these two paralyzing times to assess the impact of after pulses.

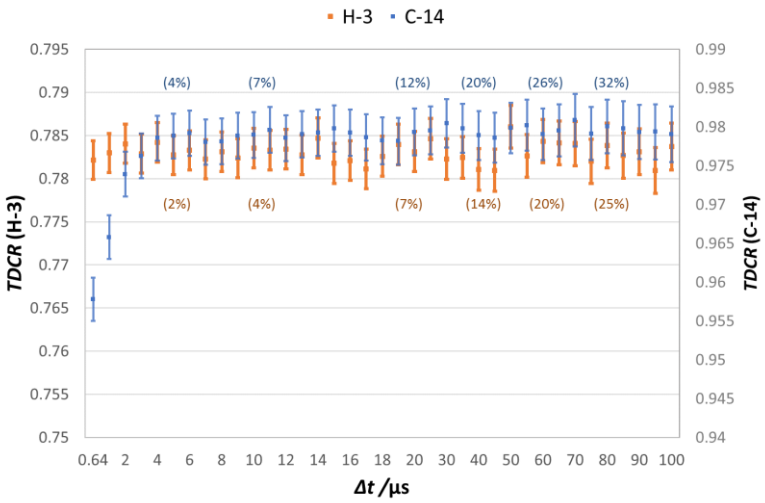

Fig. 9 *TDCR* value as a function of the extended dead time for the two sources of ^{3}H and ^{14}C. The measurement dead time is displayed in brackets.

c. Setup of the coincidence resolving time

The resolution time $\Delta\tau$ is the time window during which any triggering between the two or three channels will be considered as a double or triple coincident event. Too short a $\Delta\tau$ leads to a risk of non-detection. Conversely, too long a resolution time increases the risk of accidental coincidences. Keeping the same experimental configuration as before, the evolution of the *TDCR* value as a function of the resolving time is studied. It is observed in Fig. 10 a disparity of behaviour between ^{3}H and ^{14}C with the resolving time. While the *TDCR* value of ^{14}C reaches a constant (or slightly decreasing) value from a resolution time greater than 30 ns, the *TDCR* value associated with ^{3}H increases monotonically. This can be explained by the fact that the stopping power of very low energy electrons is

greater than for higher energy electrons. The decays of tritium nuclei will therefore have a greater tendency to produce triplet states of excitement leading to delayed fluorescence or phosphorescence [37]. Anyway, this phenomenon depending on the scintillating liquid, concerns almost exclusively low energy emitting isotopes such as ^{55}Fe or tritium. Although it can potentially cause a bias in the context of primary measurements, these biases are constant for a given scintillator and can therefore be assumed in ESIR operation. So, a value of $\Delta\tau$ equal to 50 ns will be considered whatever the radionuclide is. This choice guarantees a margin compared to the minimum of 30 ns observed here and greatly minimizes the risk of accidental coincidence. A measurement with a resolution time of 100 ns will also be simultaneously recorded in order to control the stability of the scintillating liquid with respect to the phenomenon described above.

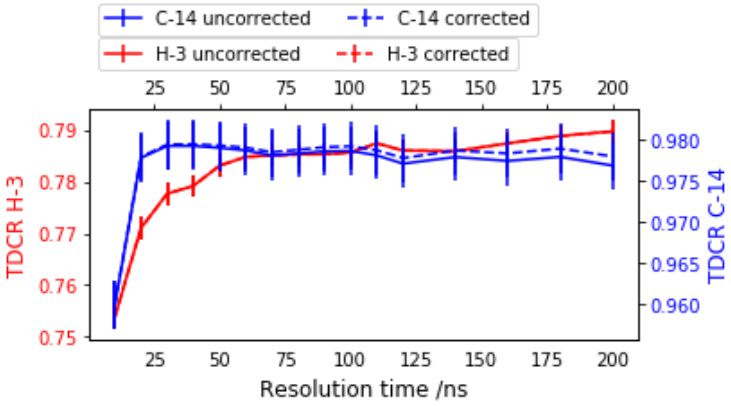

Fig. 10 *TDCR* value as a function of the coincidence resolving time for the two sources of ^{3}H and ^{14}C.

5. The quality assurance

The quality assurance will play a critical role to control the long-term reproducibility of the reference values produced by the ESIR. A set of procedures were established and specific attention was carried on the automation of the measurement analysis by a Python program and by establishing a Git-controlled database in the same framework as it was recently established for the SIR [7].

Besides, a monthly periodic control of the system was setup since its commissioning in August 2020. The check sources are 6 toluene-based LS sources (^{14}C sources and ^{3}H sources) known for their good stability other a long-term period. The reproducibility of the ESIR is assessed by performing statistical analysis on these quality measurements. As recommended by the ISO17025:2017, control charts (x-chart, R-chart, CUSUM chart and EWMA chart) are applied to detect outliers or drifts signing that the system is no under statistical control. Also, the consistency of the data set with the uncertainty evaluation of each point is tested using a Chi-squared test.

The results for one of the tritium sources for which a first measurement point was obtained in March 2020 are displayed in Figs. 11-14. The error bars are standard uncertainty associated with the measurement points, x_i. The lower end upper control limits are the mean of all the measurement points +/- 2 times (yellow lines) or 3 times (red lines) standard deviation (type A evaluation). The central red line represents the mean with a thickness equal to +/- 1 standard deviation of the mean value.

The raw comparison indicator I_0 and the *TDCR* values (Figs. 11 and 12) show clearly that the system is not by itself stable. Even if the raw measurement data I_0 passes tests from control charts, it fails the Chi-squared test with a p-value equal to 0.002 (corresponding to a Birge ratio equal to 1.76). So, the hypothesis of consistency of the measurements according to their individual uncertainty evaluations can be rejected with a 95 % confidence level. This means that it exists slight (about 0.2 %) but significant drifts in the detection efficiency that are not taken into account in the uncertainty budget.

For the same data set, key comparison comparison indocators I_1 and the I_2 are displayed in Fig. 13 and Fig. 14. They both pass tests from control charts and the Chi-squared test with p-values close to 1. This result stresses the robustness provided by the approach developed for the ESIR. It demonstrates that the ESIR is capable to provide reproducible values I_1 and I_2 during a period of 20 months.

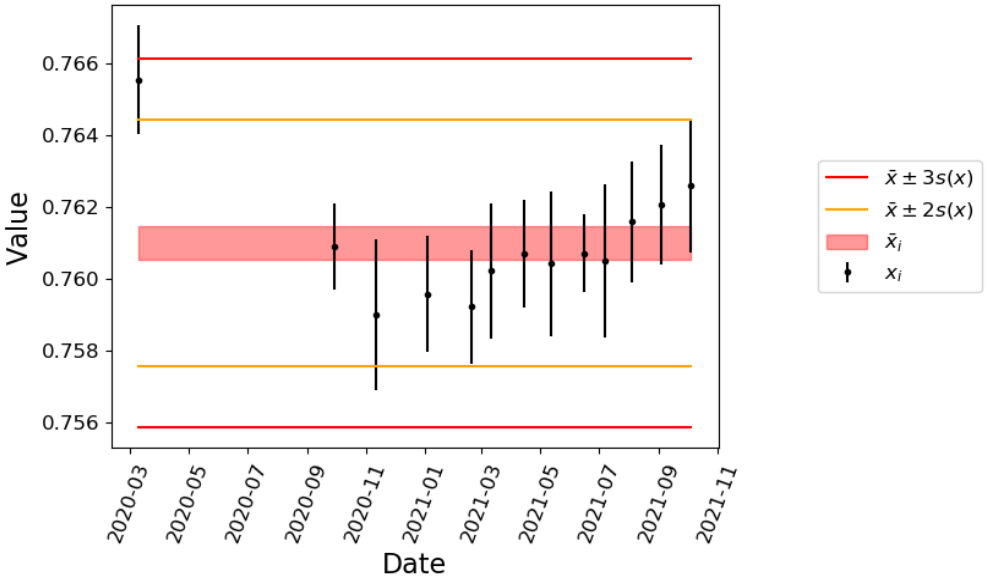

377

378 **Fig. 11** *TDCR* values obtained for the ^{3}H source HDCO since March 2020

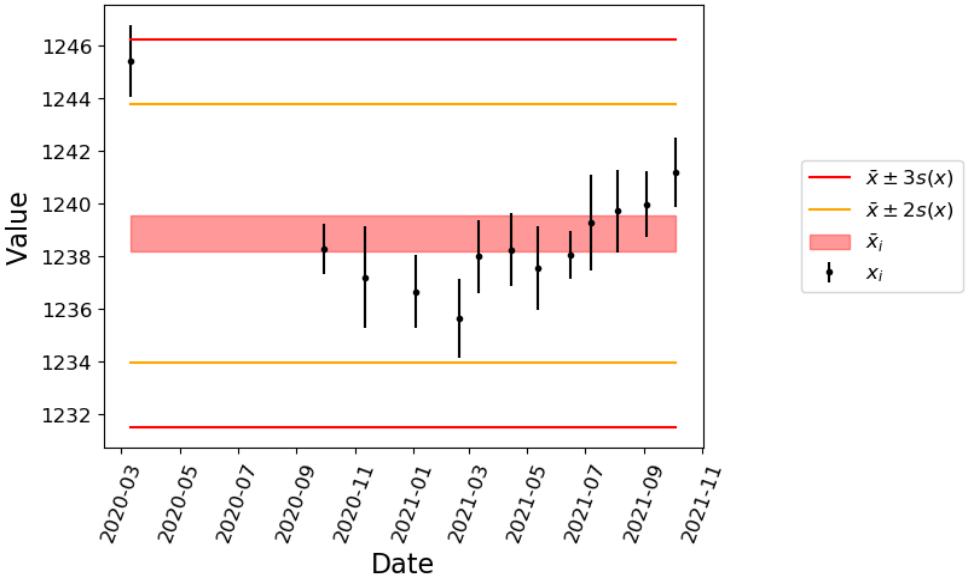

379

380 **Fig. 12** I_0 values obtained for the ^{3}H source HDCO since March 2020

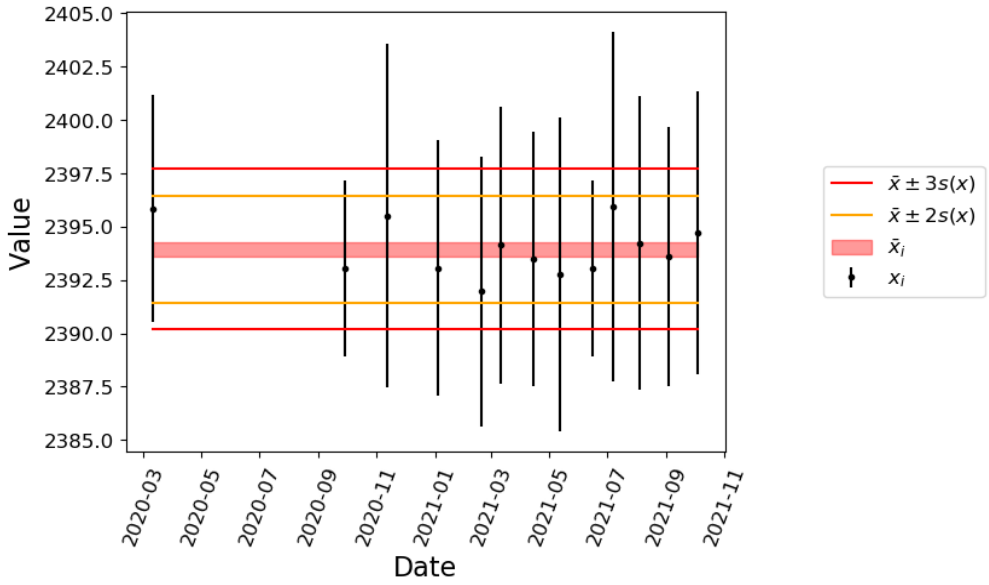

381

382 **Fig. 13** I_1 values obtained for the ^{3}H source HDCO since March 2020

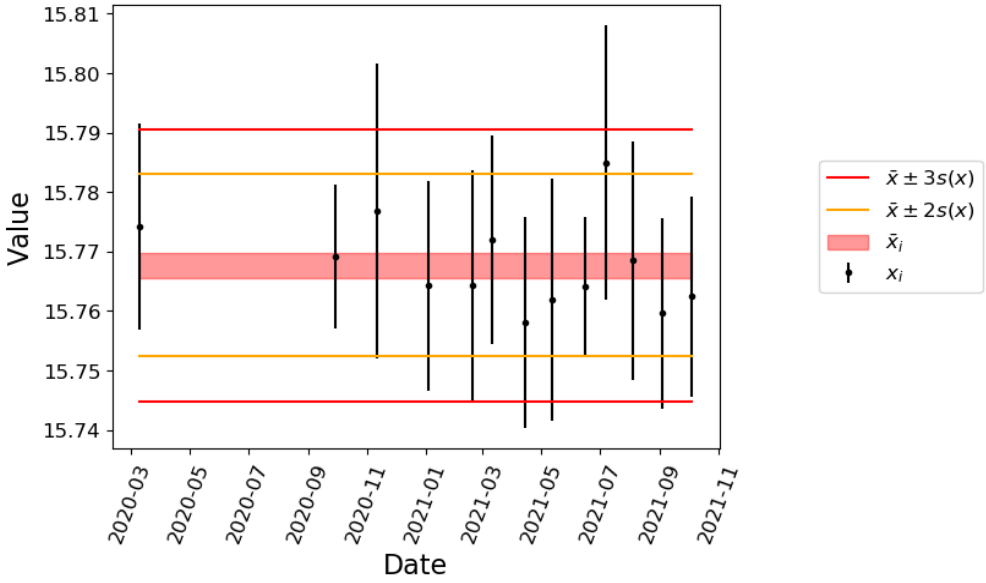

383

384 **Fig. 14** I_2 values obtained for the ^{3}H source HDCO since March 2020

385 Results for the other check standards are available as supplementary information.

386

Conclusions

A liquid scintillation source facility and a new TDCR system have been set up at the BIPM to extend the SIR to pure alpha-, pure beta-emitting and some electron capture-decaying radionuclides. The objective is to improve the traceability chain for radionuclides of interest for new cancer treatments and some environmental issues.

The service was commissioned in August 2020. Since this data, the ESIR operates, through a set of procedures and fixed defined parameters, to produce highly reproducible measurement quantities. These quantities called key comparison indicators will permit to establish reference refence values (KCRV) for these radionuclides and degrees of equivalence for the participating NMI/DIs. The ESIR aims to be an on-demand service for at least isotope emitting medium and high energy particles. A CCRI(II) pilot study on Co-60 key comparison is underway to validate the ESIR against the SIR in the context of an international key comparison exercise. This pilot study implies 12 NMI/DIs and is planned to be completed in 2022.

Meantime, the periodic quality control using toluene-based liquid scintillation sources of ^{3}H and ^{14}C have been launched. They have permitted to demonstrate the capability of the ESIR to produce key comparison indicators with a good reproducibility for a 20-month period. This preliminary result is encouraging on the stability attainable by the unique method of the ESIR based on the TDCR technique.

Many challenges and perspectives are under study with ESIR such as,

- the adaptation of the source preparation facility to address alpha-emitting radionuclides (e.g., ^{211}At, ^{212}Bi, ^{212}Pb, ^{213}Bi, ^{227}Th),
- the set-up of a redundant digital signal processing,
- the development of an LS cocktail prepared at the BIPM to allow on demand comparison for radionuclides emitting low energy particles (e.g., ^{55}Fe, ^{63}Ni, ^{3}H and ^{241}Pu),

- the development of a transportable ESIR (analog to the SIRTI) using the transportable TDCR system developed by the LNE/LNHB [38].

References

[1] CIPM 2003 Mutual recognition of national measurement standards and of calibration and measurement certificates issued by national metrology institutes

[2] Karam L R 2007 Application of the CIPM MRA to radionuclide metrology *Metrologia* **44** 4–9

[3] Rytz A 1983 The international reference system for activity measurements of γ-ray emitting nuclides *Int. J. Appl. Radiat. Isot.* **34** 1047–56

[4] Ratel G 2007 The Système International de Référence and its application in key comparisons *Metrologia* **44** 7–16

[5] Karam L, Judge S and Louw W 2019 The international measurement system for radionuclide metrology: A strategy for the future *Appl. Radiat. Isot.* **154** 108838

[6] Michotte C, Nonis M, Bobin C, Altzizoglou T and Sibbens G 2013 *The SIRTI: a new tool developed at the BIPM for comparing activity measurements of short-lived radionuclides world-wide*

[7] Coulon R, Courte S, Judge S, Michotte C and Nonis M 2021 Digitalization of the reporting of key comparisons for radionuclide metrology *Meas. Sci. Technol.* **Submitted** 113015

[8] Sgouros G, Bodei L, McDevitt M R and Nedrow J R 2020 Radiopharmaceutical therapy in cancer: clinical advances and challenges *Nat. Rev. Drug Discov.* **19** 589–608

[9] Parker C, Lewington V, Shore N, Kratochwil C, Levy M, Lindén O, Noordzij W, Park J and Saad F 2018 Targeted Alpha Therapy, an Emerging Class of Cancer

Agents *JAMA Oncol.* **4** 1765

[10] Duchemin C, Ramos J P, Stora T, Ahmed E, Aubert E, Audouin N, Barbero E, Barozier V, Bernardes A-P, Bertreix P, Boscher A, Bruchertseifer F, Catherall R, Chevallay E, Christodoulou P, Chrysalidis K, Cocolios T E, Comte J, Crepieux B, Deschamps M, Dockx K, Dorsival A, Fedosseev V N, Fernier P, Formento-Cavaier R, El Idrissi S, Ivanov P, Gadelshin V M, Gilardoni S, Grenard J-L, Haddad F, Heinke R, Juif B, Khalid U, Khan M, Köster U, Lambert L, Lilli G, Lunghi G, Marsh B A, Palenzuela Y M, Martins R, Marzari S, Menaa N, Michel N, Munos M, Pozzi F, Riccardi F, Riegert J, Riggaz N, Rinchet J-Y, Rothe S, Russell B, Saury C, Schneider T, Stegemann S, Talip Z, Theis C, Thiboud J, van der Meulen N P, van Stenis M, Vincke H, Vollaire J, Vuong N-T, Webster B, Wendt K and Wilkins S G 2021 CERN-MEDICIS: A Review Since Commissioning in 2017 *Front. Med.* **8**

[11] Iravani A, Violet J, Azad A and Hofman M S 2020 Lutetium-177 prostate-specific membrane antigen (PSMA) theranostics: practical nuances and intricacies *Prostate Cancer Prostatic Dis.* **23** 38–52

[12] Michotte C, Ratel G, Courte S, Johansson L, Keightley J, Arinc A, Bakhshandeiar E, Pommé S, Altzitzoglou T, Paepen J and Van Ammel R 2014 BIPM comparison BIPM.RI(II)-K1.Lu-177 of activity measurements of the radionuclide 177 Lu for the NPL (UK) and the IRMM (EU), with linked results for the comparison CCRI(II)-K2.Lu-177 *Metrologia* **51** 06002–06002

[13] Michotte C, Courte S, Nonis M, Coulon R, Judge S, Kossert K and Nähle O 2021 Final report of the new BIPM comparison BIPM.RI(II)-K1.Ac-225 of activity measurements of the radionuclide 225 Ac to include the 2019 result of the PTB (Germany) *Metrologia* **58** 06018

[14] Michotte C, Courte S, Nonis M, Coulon R, Judge S, Ratel G, Fréchou C, Cassette P, Keightley J, Kossert K and Nähle O 2021 Final report of the new BIPM comparison BIPM.RI(II)-K1.Ra-223 of activity measurements of the radionuclide

223 Ra including the 2014 result of the NPL (United Kingdom), the 2014 result of the PTB (Germany) and the 2018 result of the LNE-LNHB (France) *Metrologia* **58** 06007

[15] Wallenius M, Lützenkirchen K, Mayer K and Varga Z 2018 Actinides: Nuclear Forensics *Encyclopedia of Inorganic and Bioinorganic Chemistry* (Chichester, UK: John Wiley & Sons, Ltd) pp 1–17

[16] Jiang J, Davies A, Thorne K and Gilligan C 2017 Rapid analysis of 89Sr and 90Sr in nuclear forensics samples *J. Radioanal. Nucl. Chem.* **311** 1417–25

[17] Jiang J, Davies A V. and Britton R E 2017 Measurement of 160Tb and 161Tb in nuclear forensics samples *J. Radioanal. Nucl. Chem.* **314** 727–36

[18] Pochwalski K, Broda R and Radoszewski T 1988 Standardization of pure beta emitters by liquid-scintillation counting *Int. J. Radiat. Appl. Instrumentation. Part* **39** 165–72

[19] Broda R 2003 A review of the triple-to-double coincidence ratio (TDCR) method for standardizing radionuclides *Appl. Radiat. Isot.* **58** 585–94

[20] Nedjadi Y, Duc P F, Bochud F and Bailat C 2016 On the stability of 3H and 63Ni Ultima Gold liquid scintillation sources *Appl. Radiat. Isot.* **118** 25–31

[21] Coulon R, Broda R, Cassette P, Courte S, Jerome S, Judge S, Kossert K, Liu H, Michotte C and Nonis M 2020 The international reference system for pure β-particle emitting radionuclides: an investigation of the reproducibility of the results *Metrologia* **57** 035009

[22] Coulon R, Judge S, Liu H and Michotte C 2021 The international reference system for pure beta-particle emitting radionuclides: an evaluation of the measurement uncertainties *Metrologia* **58** 025007

[23] Kossert K, Sabot B, Cassette P, Coulon R and Liu H 2020 On the photomultiplier-tube asymmetry in TDCR systems *Appl. Radiat. Isot.* **163** 109223

[24] Broda R, Bonková I, Capogni M, Carconi P, Cassette P, Coulon R, Courte S, Felice P De, Dziel T, Fazio A, Frechou C, Galea R, García-Toraño E, Kołakowska E, Kossert K, Krivošík M, Lech E, Lee K B, Liang J, Listkowska A, Liu H, Navarro N, Nähle O J, Nowicka M, Rooy M van, Sabot B, Saganowski P, Sato Y, Tymiński Z, Yunoki A, Zhang M and Ziemek T 2021 The CCRI(II)-K2.Fe-55.2019 key comparison of activity concentration measurements of a 55 Fe solution *Metrologia* **58** 06010

[25] EURAMET 2015 *Guidelines on the calibration of non-automatic weighing instruments*

[26] Lourenço V and Bobin C 2015 Weighing uncertainties in quantitative source preparation for radionuclide metrology *Metrologia* **52** S18–29

[27] Bobin C and Bouchard J 2006 A 4π(LS)β-γ coincidence system using a TDCR apparatus in the β-channel *Appl. Radiat. Isot.* **64** 124–30

[28] Cassette P and Do P 2008 The Compton source efficiency tracing method in liquid scintillation counting: A new standardization method using a TDCR counter with a Compton spectrometer *Appl. Radiat. Isot.* **66** 1026–32

[29] Anon ODM98-B

[30] Xiaoguang Zhong, Li Yu, Jiazhen Sun and Yuefang Zhang 1993 Radiation stability of PTFE irradiated under various conditions *Polym. Degrad. Stab.* **39** 187–91

[31] Mitev K, Cassette P, Jordanov V, Liu H R and Dutsov C 2017 Design and performance of a miniature TDCR counting system *J. Radioanal. Nucl. Chem.* **314** 583–9

[32] Jordanov V, Cassette P, Dutsov C and Mitev K 2020 Development and applications of a miniature TDCR acquisition system for in-situ radionuclide metrology *Nucl. Instruments Methods Phys. Res. Sect. A Accel. Spectrometers, Detect. Assoc. Equip.* **954** 161202

[33] Bouchard J and Cassette P 2000 MAC3: An electronic module for the processing of pulses delivered by a three photomultiplier liquid scintillation counting system *Appl. Radiat. Isot.* **52** 669–72

[34] Dutsov C, Cassette P, Sabot B and Mitev K 2020 Evaluation of the accidental coincidence counting rates in TDCR counting *Nucl. Instruments Methods Phys. Res. Sect. A Accel. Spectrometers, Detect. Assoc. Equip.* **977** 164292

[35] Michotte C, Courte S, Nonis M, Coulon R, Judge S, Nälhle O and Takács M P 2021 Update of the BIPM comparison BIPM.RI(II)-K1.Sr-85 of activity measurements of the radionuclide 85 Sr to include the 2018 result of the PTB (Germany) *Metrologia* **58** 06006

[36] Akgun U, Ayan A S, Aydin G, Duru F, Olson J and Onel Y 2008 Afterpulse timing and rate investigation of three different Hamamatsu Photomultiplier Tubes *J. Instrum.* **3** T01001–T01001

[37] Bobin C, Thiam C, Chauvenet B and Bouchard J 2012 On the stochastic dependence between photomultipliers in the TDCR method *Appl. Radiat. Isot.* **70** 770–80

[38] Anon Discussion with Benoit Sabot, 2021

Supplementary information

The full analysis of the period quality control is reported in this appendix. The error bars are standard uncertainty associate with the measurement points, x_i. The lower end upper control limits are the mean of all the measurement points +/- 2 times (yellow lines) or 3 times (red lines) standard deviation (type A evaluation). The central red line represents the mean with a thickness equal to +/- 1 standard deviation of the mean value.

a. Toluene-based tritium standard HDCO

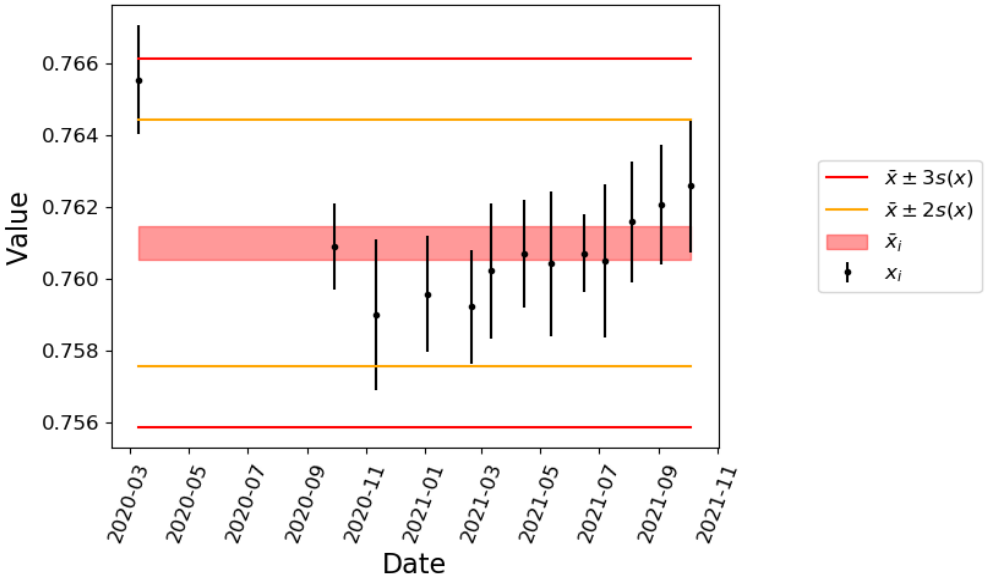

Fig. 1 *TDCR* values obtained for the ^{3}H source HDCO since March 2020

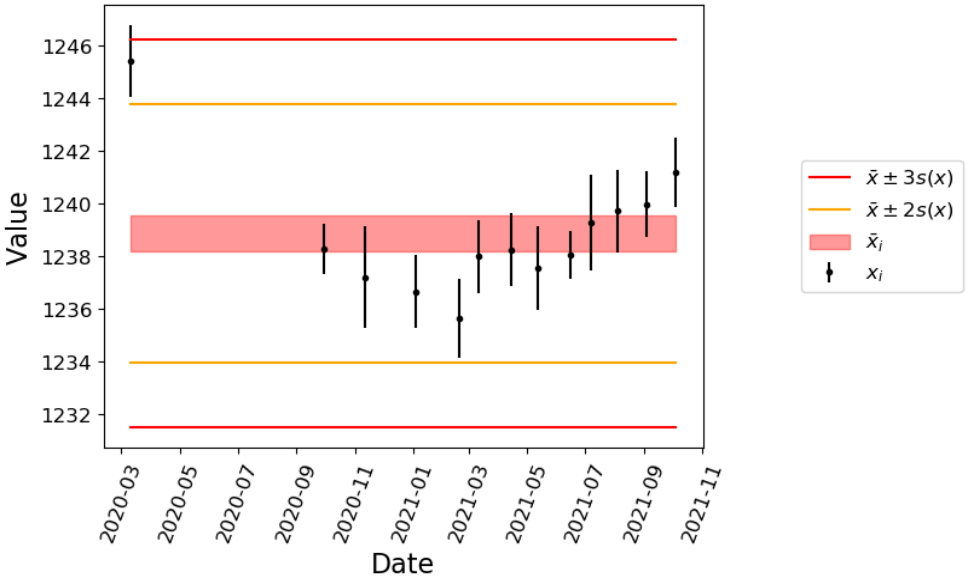

Fig. 3 I_0 values obtained for the ^{3}H source HDCO since March 2020

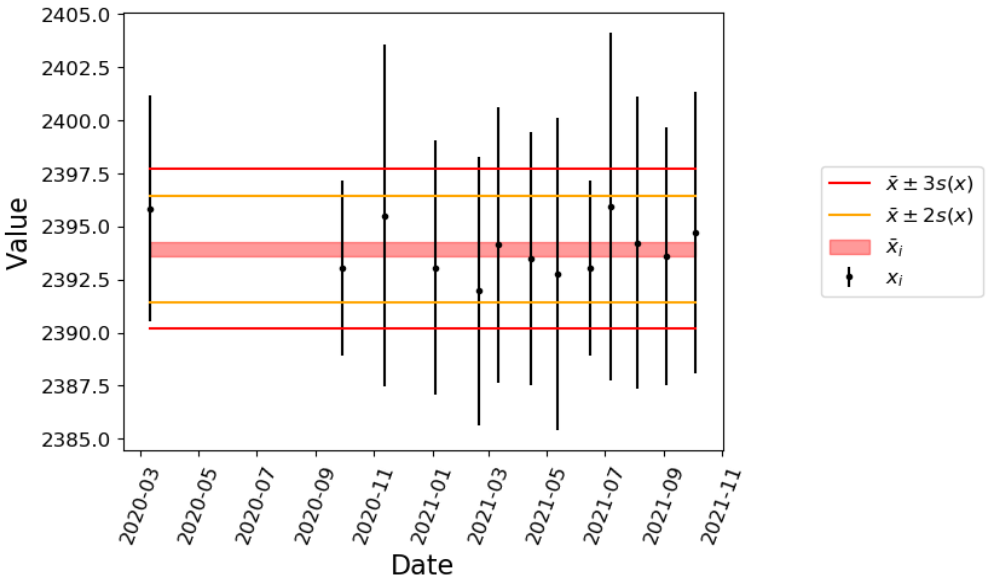

Fig. 2 I_1 values obtained for the ^{3}H source HDCO since March 2020

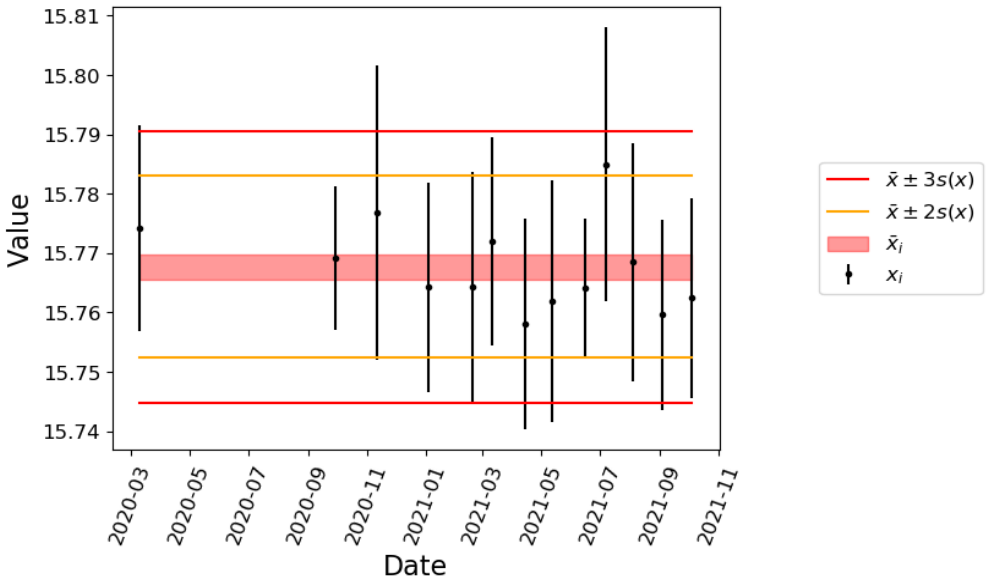

Fig. 2 I_2 values obtained for the ^{3}H source HDCO since March 2020

b. Toluene-based tritium standard HMI

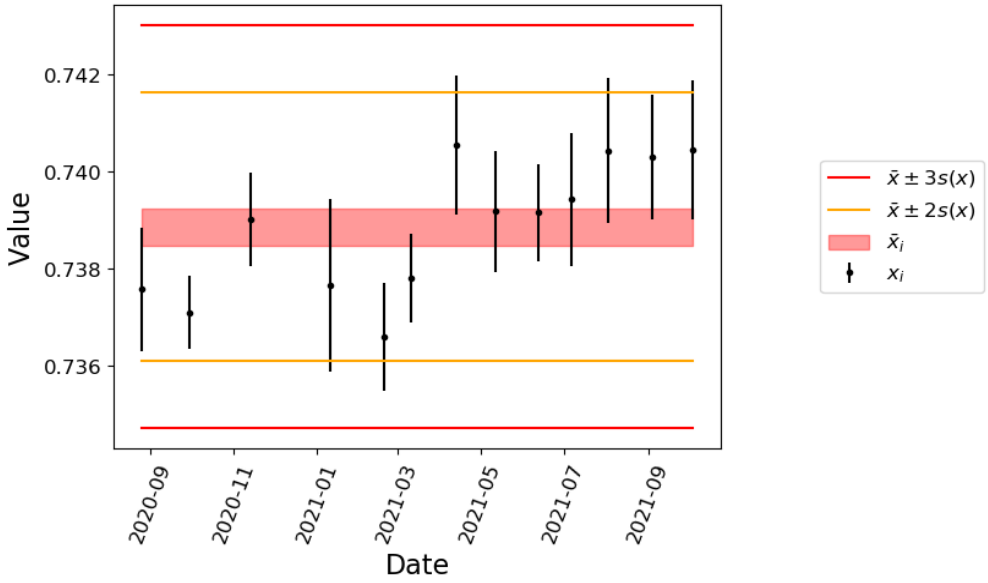

Fig. 1 *TDCR* values obtained for the ^{3}H source HMI since August 2020

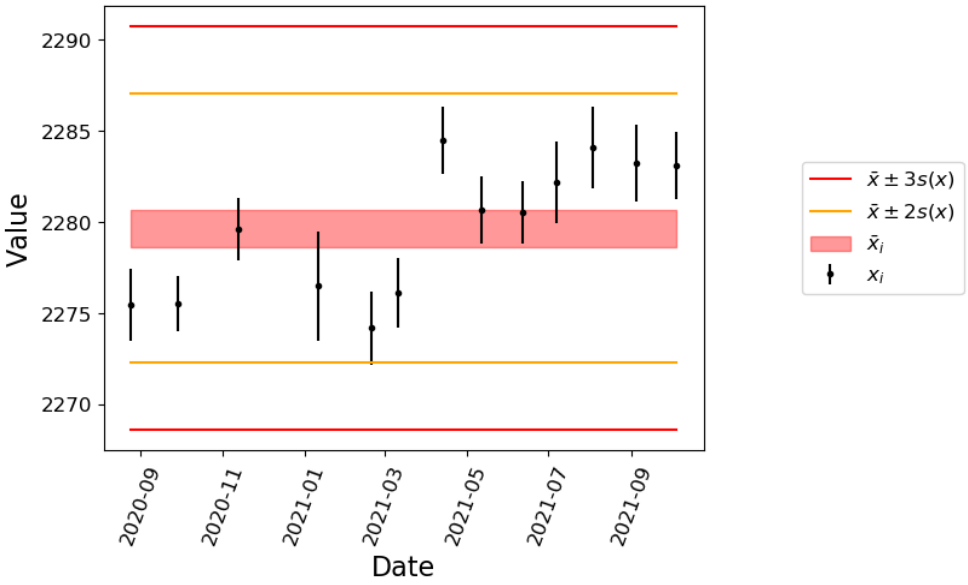

557

558 **Fig. 2** I_0 values obtained for the ^{3}H source HMI since August 2020

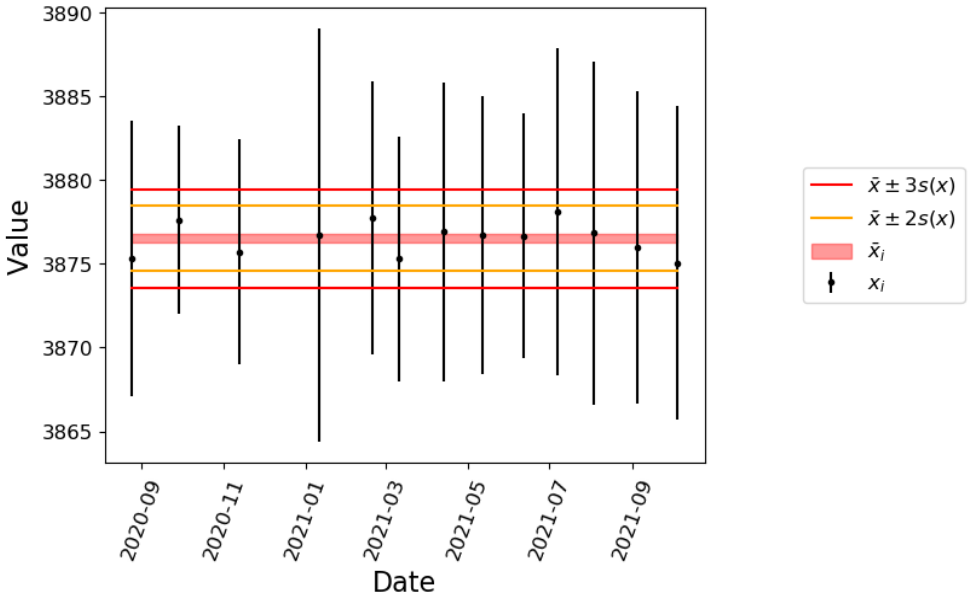

559

560 **Fig. 2** I_1 values obtained for the ^{3}H source HMI since August 2020

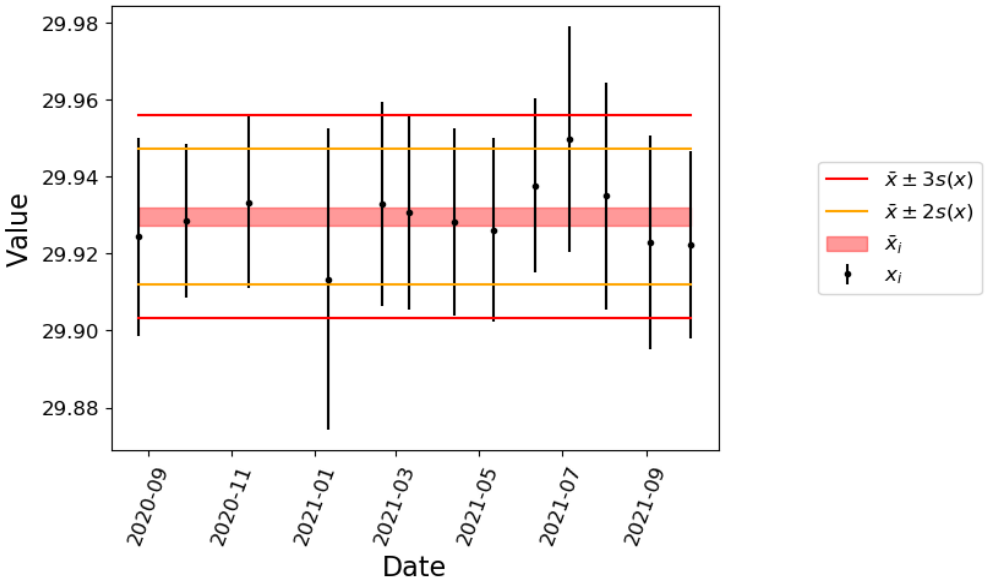

Fig. 2 I_2 values obtained for the ^{3}H source HMI since August 2020

c. Toluene-based tritium standard H3-117TOL

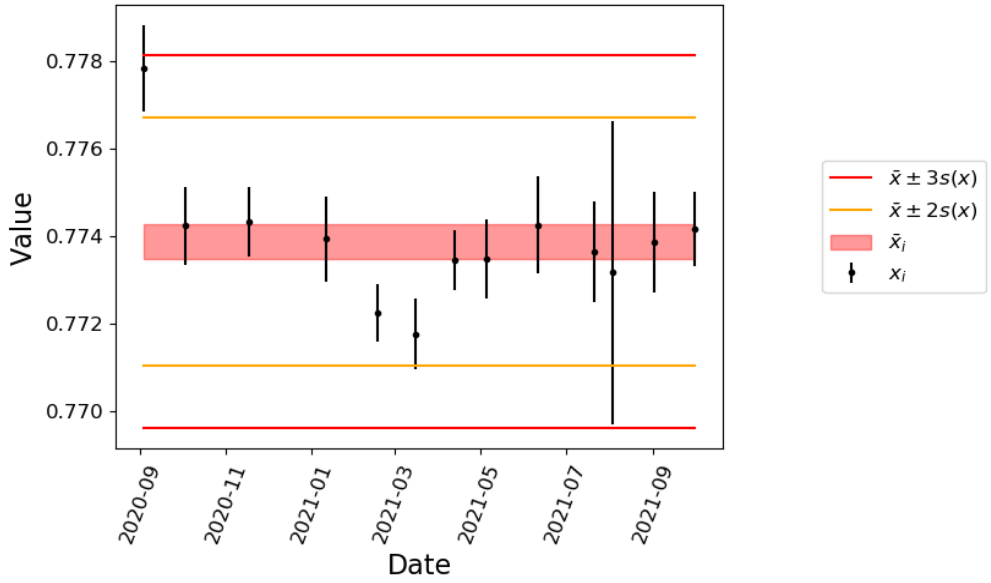

Fig. 1 *TDCR* values obtained for the ^{3}H source H3-117TOL since August 2020

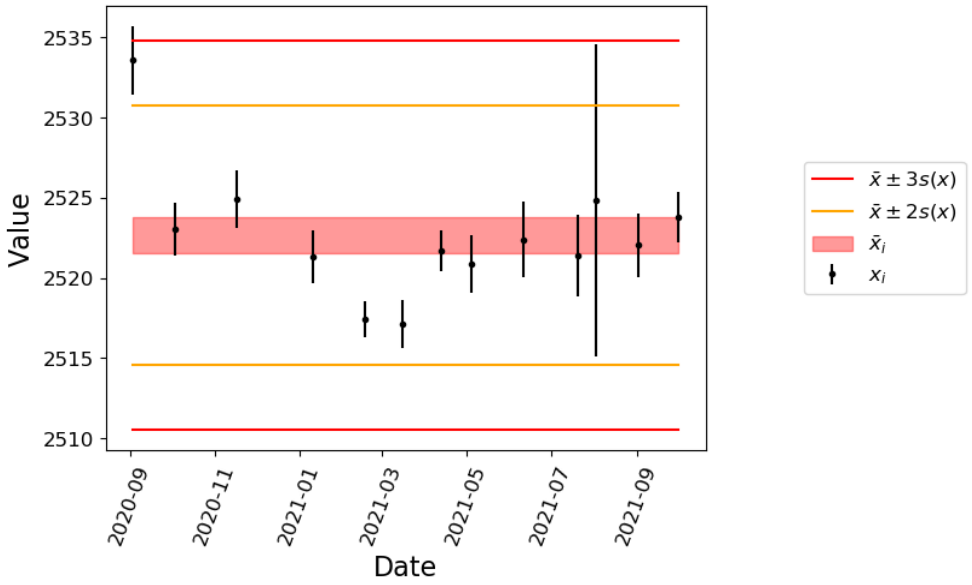

568

569 **Fig. 2** I_0 values obtained for the ^{3}H source H3-117TOL since August 2020

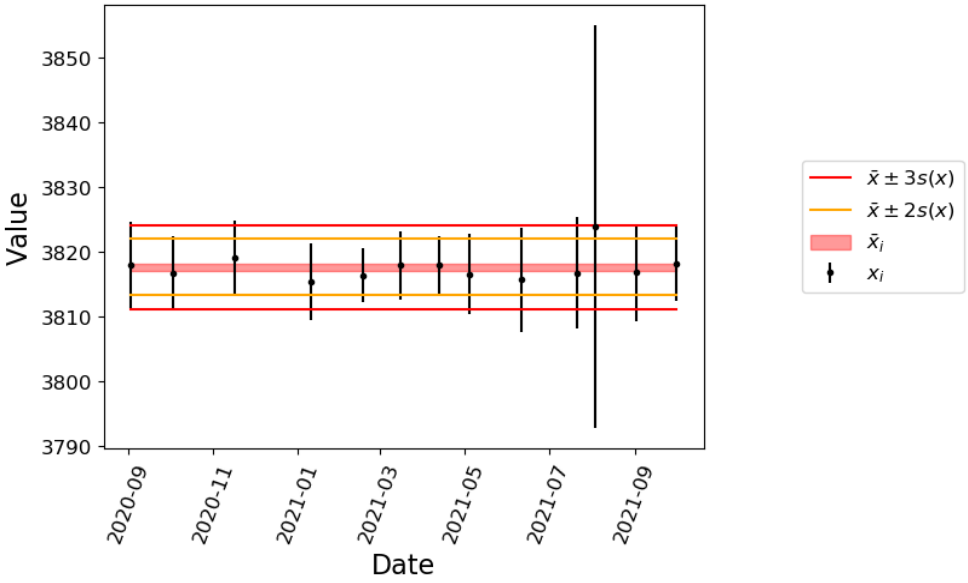

570

571 **Fig. 2** I_1 values obtained for the ^{3}H source H3-117TOL since August 2020

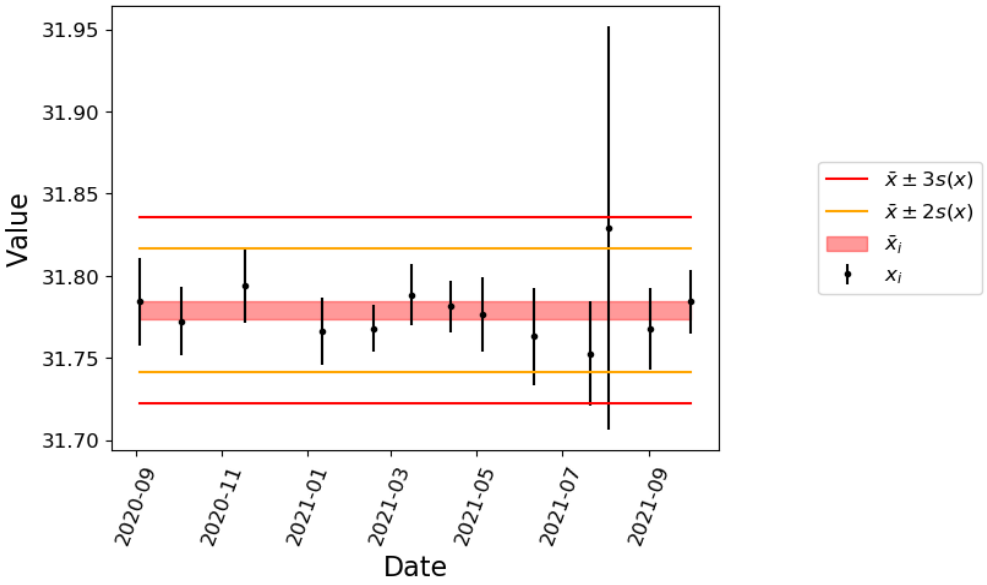

572

573 **Fig. 2** I_2 values obtained for the ^{3}H source H3-117TOL since August 2020

574

575 *d. Toluene-based 14C standard CCT*

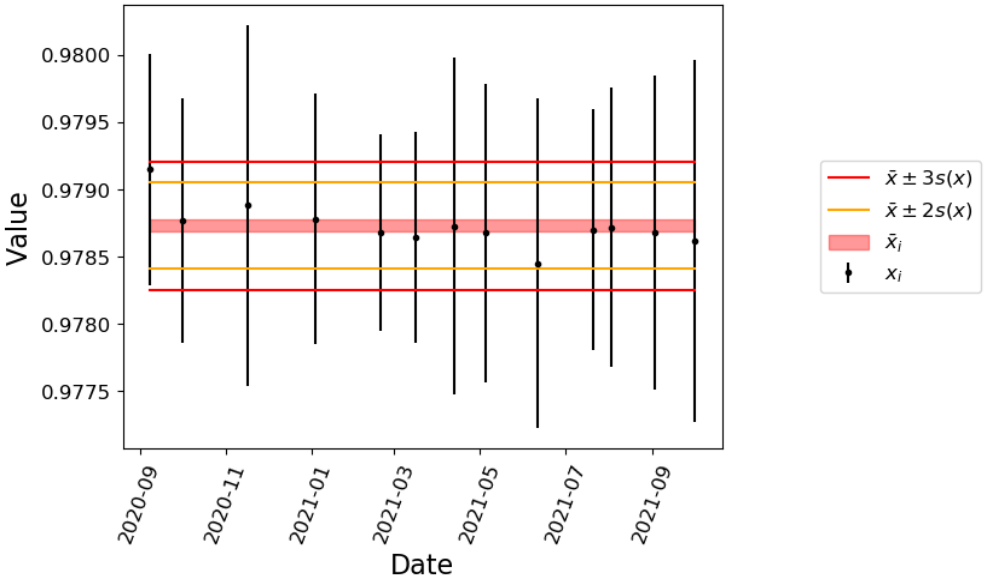

576

577 **Fig. 1** *TDCR* values obtained for the ^{14}C source CCT since August 2020

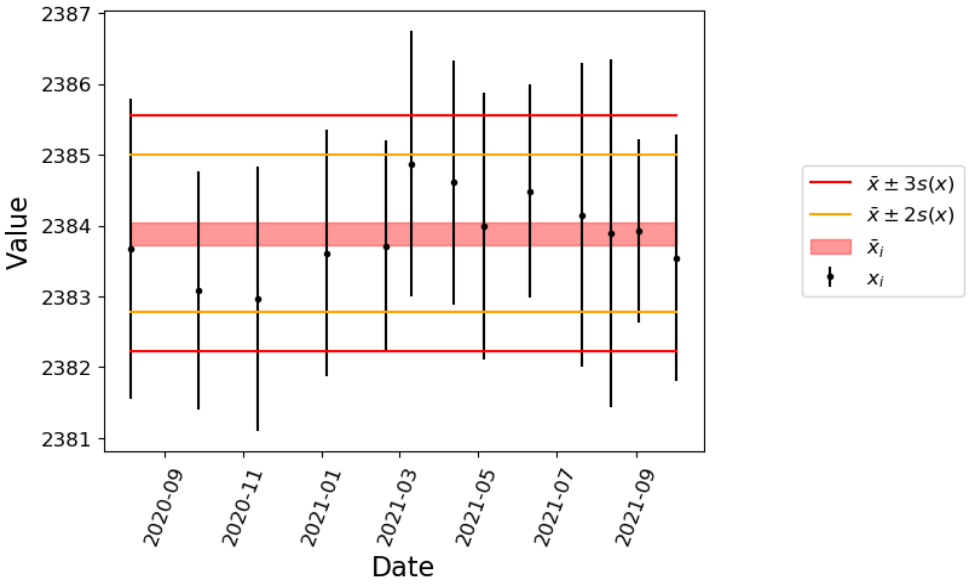

578

579 **Fig. 2** I_0 values obtained for the ^{14}C source CCT since August 2020

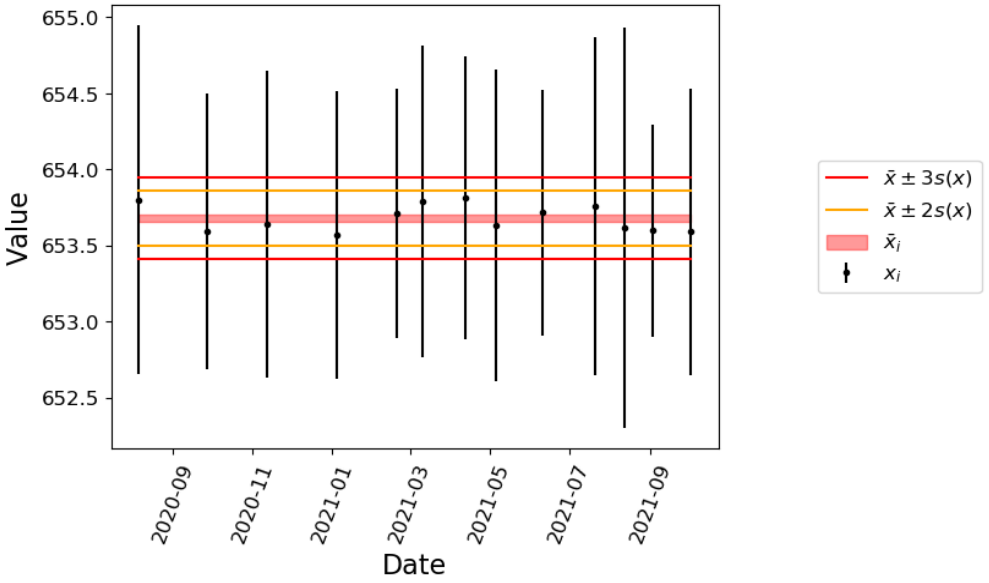

580

581 **Fig. 2** I_1 values obtained for the ^{14}C source CCT since August 2020

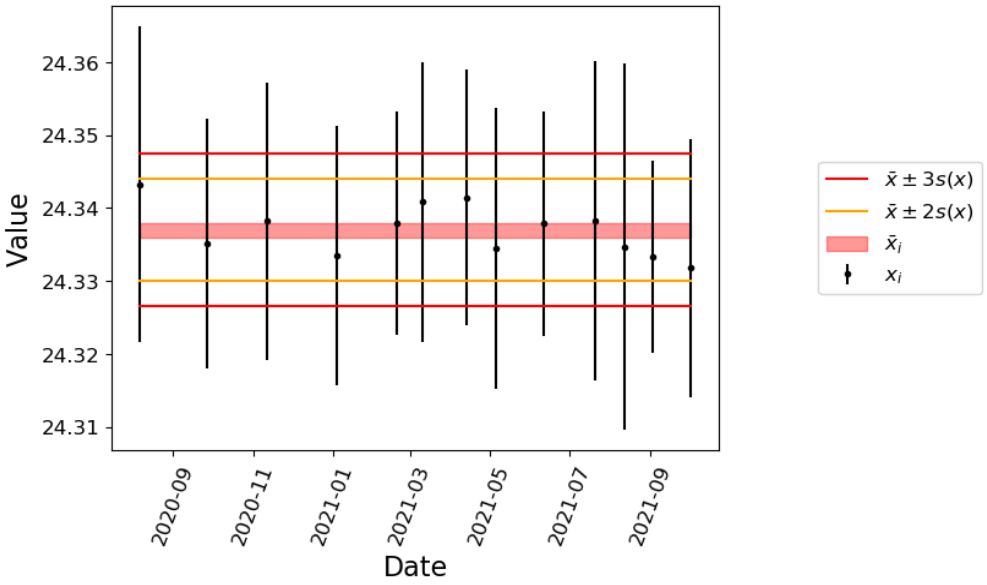

582

583 **Fig. 2** I_2 values obtained for the ^{14}C source CCT since August 2020

584

585 *e. Toluene-based 14C standard CMF*

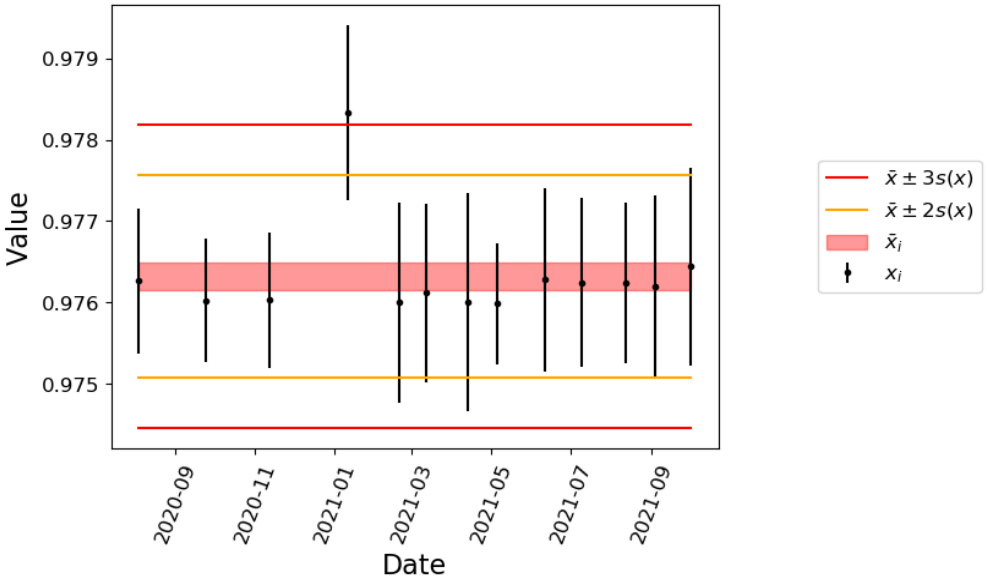

586

587 **Fig. 1** *TDCR* values obtained for the ^{14}C source CMF since August 2020

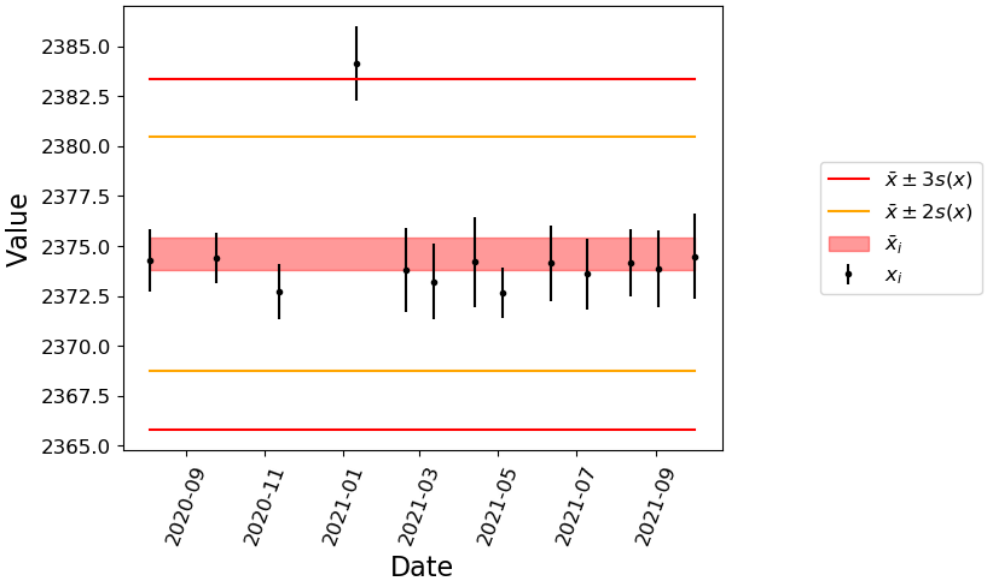

588

589 **Fig. 2** I_0 values obtained for the ^{14}C source CMF since August 2020

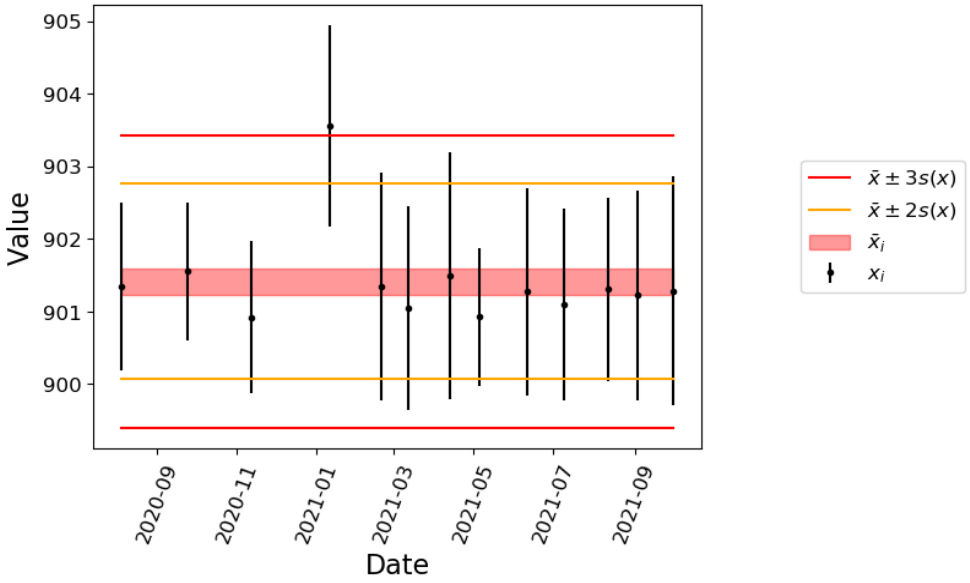

590

591 **Fig. 2** I_1 values obtained for the ^{14}C source CMF since August 2020

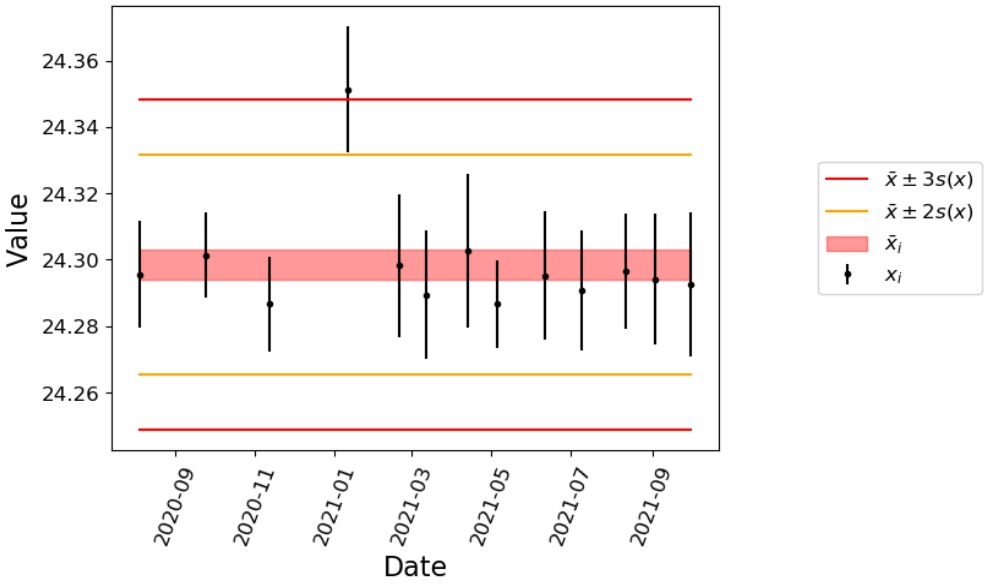

Fig. 2 I_2 values obtained for the ^{14}C source CMF since August 2020

f. Toluene-based 14C standard C14-117TOL

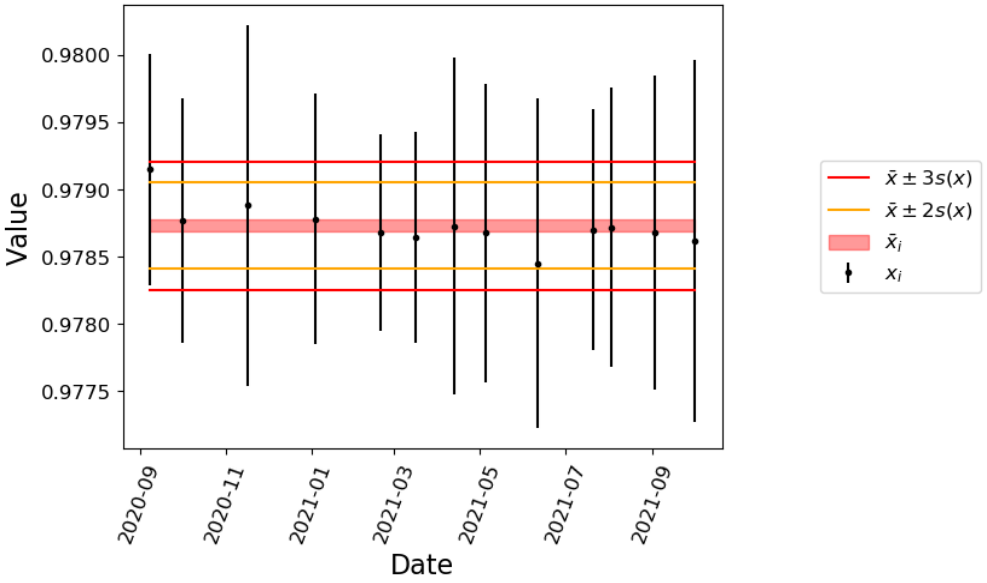

Fig. 1 *TDCR* values obtained for the ^{14}C source C14-117TOL since August 2020

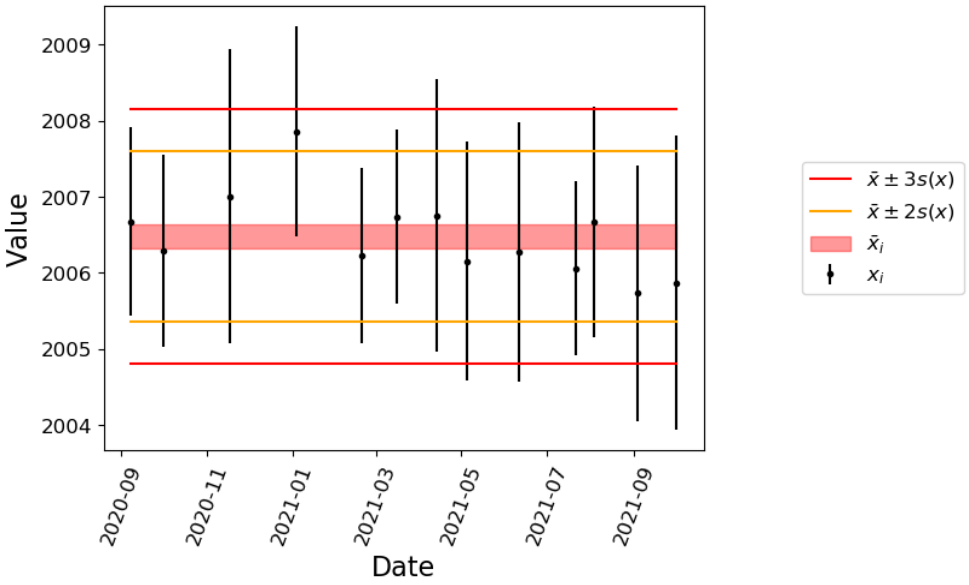

599

600 **Fig. 2** I_0 values obtained for the ^{14}C source C14-117TOL since August 2020

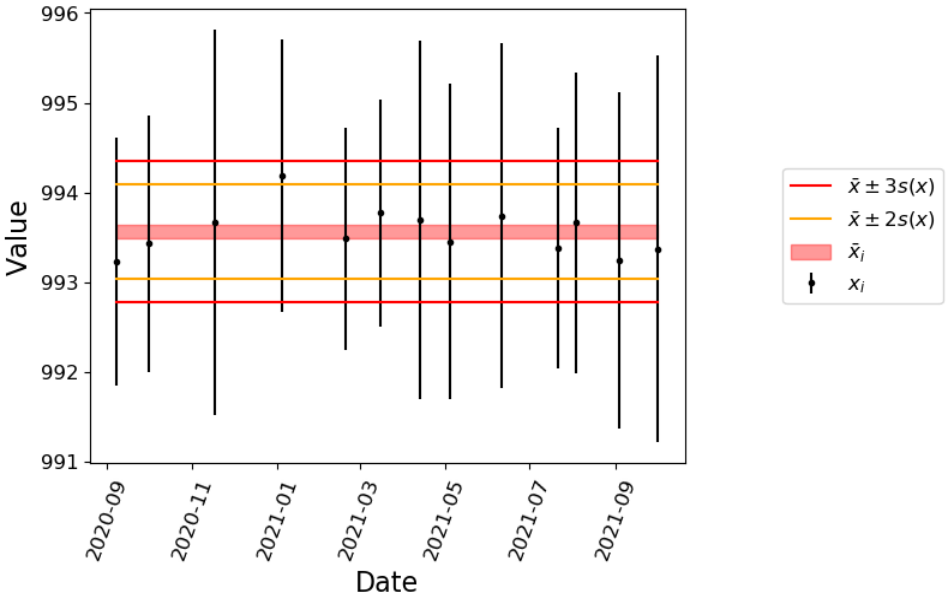

601

602 **Fig. 2** I_1 values obtained for the ^{14}C source C14-117TOL since August 2020

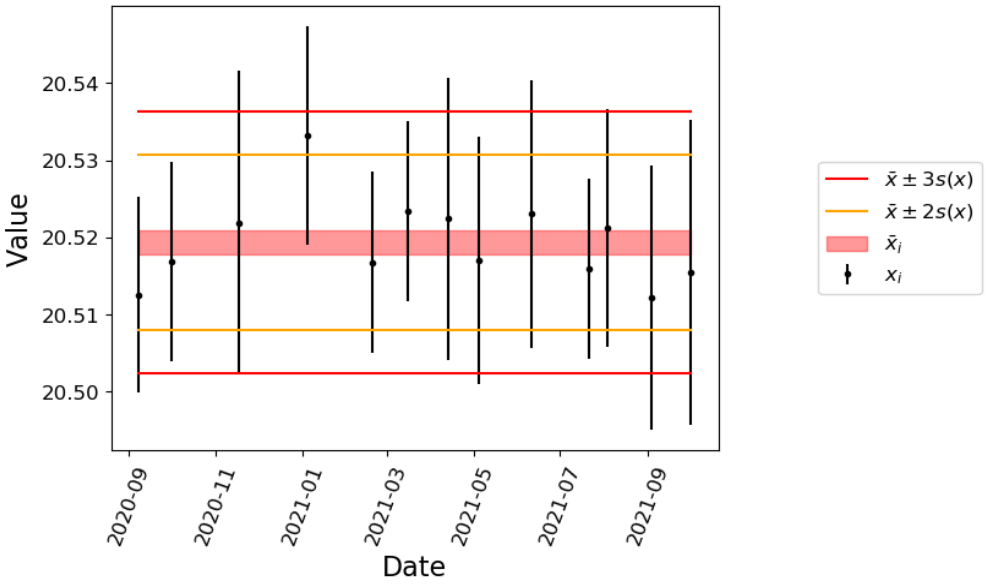

603

604 **Fig. 2** I_2 values obtained for the ^{14}C source C14-117TOL since August 2020

605